metals

MDPI

Article

Numerical Investigation and Model Recalibration for Web-Post Buckling of Stainless Steel Cellular Beams

Imane Bachguar [1,*], Ouadia Mouhat [1] and Rabee Shamass [2]

[1] Civil Engineering and Environment Laboratory (LGCE), Mohammadia Engineering School, Mohammed V University, Rabat 10090, Morocco; ouadie.mouhat@est.um5.ac.ma
[2] Department of Civil and Environmental Engineering, Brunel University London, London UB8 3PH, UK; rabee.shamass@brunel.ac.uk
* Correspondence: imane_bachguar@um5.ac.ma

Abstract

Steel cellular beams have become widely used in construction projects, particularly for long-span structures. This work focuses on stainless steel, which exhibits a nonlinear stress–strain behavior from low strain levels, without a well-defined yield plateau. Its conventional yield strength is determined at 0.2% plastic strain, followed by significant and continuous strain hardening up to failure. This mechanical characteristic directly affects the buckling resistance of structural elements, requiring the consideration of the variable tangent modulus E_t in design models. In the absence of experimental tests on stainless steel cellular beams, a finite element model was developed and validated using tests carried out on carbon steel beams. An extensive parametric study was then conducted to analyze the influence of geometry and material characteristics. In total, the analysis involved 1400 finite element models. Based on these results, the strut model was validated for the seven stainless steel grades considered. Subsequently, recalibrated values of the coefficient C_2 were proposed and made it possible to adjust the tangent modulus E_t in the theoretical model. The new recalibrated coefficients are directly applicable to design formulations and extend the scope of application of the strut model to stainless steel cellular beams, with good predictive accuracy.

Keywords: cellular beams; stainless steel; web-post buckling; finite element analysis; coefficient recalibration

1. Introduction

Steel cellular beams are widely used in steel construction due to their multifunctional advantages [1,2]. A key feature is the ability to achieve long spans while integrating building services within the beam depth. This integration not only allows for a more optimized use of floor space but also reduces the overall construction height and offers significant architectural flexibility.

These cellular beams are manufactured by first cutting and then re-welding a rolled I-section. The use of this manufacturing method makes it possible to obtain lightweight and resistant cellular beams, ideal for architectural and structural applications. Figures 1 and 2 illustrate the main dimensional characteristics of cellular beams. In particular, H represents the total height of the cellular beam, d_o the diameter of the opening, and s the centre-to-centre spacing between the openings.

Check for updates

Academic Editors: Shuwen Wen, Yongle Sun and Xin Chen

Received: 12 October 2026
Revised: 11 November 2026
Accepted: 12 November 2026
Published: 14 November 2026

Copyright: © 2026 by the authors. Licensee MDPI, Basel, Switzerland. This article is an open access article distributed under the terms and conditions of the Creative Commons Attribution (CC BY) license.

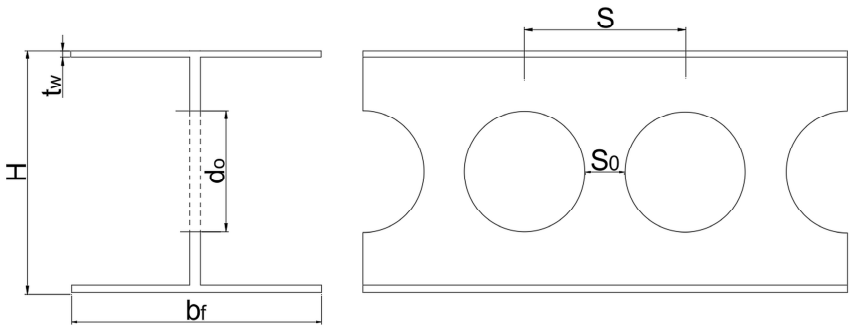


Figure 1. Cellular beam geometry.

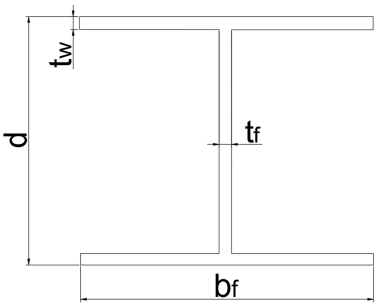


Figure 2. Parent I-beam section.

The presence of these openings modifies the load paths within the cellular beams, which alters their structural behavior. This modification introduces several failure mechanisms, such as Vierendeel bending, lateral torsional buckling and, most critically, web-post buckling. To determine the dominant failure mode, several numerical and experimental studies were conducted. These studies converge to identify web-post buckling as the dominant failure mode, particularly for cases with low spacing ratios [3,4].

Several design methods have been developed to calculate the web-post buckling (WPB) of carbon steel cellular beams. First, the approach proposed by the SCI in Publication 100 [5] develops several practical rules that allow the calculation of the shear resistance of web-posts. Subsequently, Lawson et al. [2] proposed models based primarily on the compressed strut analogy. This model was then improved by Panedpojaman et al. [6] by modifying the effective length of the strut while taking into account boundary conditions. In order to validate the new design equations, 390 models were developed. Furthermore, some studies have been based on results obtained from finite element analysis (FEA) to propose empirical resistance curves [7,8]. In addition, Tsavdaridis and D'Mello [3] based their work on 225 parametric studies carried out on beams with various opening shapes to develop a new empirical formula. Grilo et al. [9] proposed new resistance curves for web-post shear, based on finite element analysis and validated by experimental tests. Moreover, Erdal and Saka [7] aimed to maximize the load-carrying capacity of the cellular beam and minimize its weight by incorporating optimization methods. Shamass and Guarracino [10], in turn, developed an approach that does not rely on a fixed geometry but successively modifies the material and geometry properties of the web-post.

All the experimental and numerical works carried out have contributed to a good understanding of the behavior of carbon steel cellular beams and to the proposal of design methods for web-post buckling. However, these studies were conducted on carbon steel grades. Nevertheless, stainless steel is increasingly used as a primary material for load-bearing structures. This is mainly due to its mechanical performance, which is far superior to that of carbon steel, its corrosion resistance, as well as its high durability [11].

Despite the growing popularity of stainless steel in construction, the web-post buckling response of cellular beams made from this material has not been extensively investigated. One of the main reasons lies in the distinctive mechanical behavior exhibited by stainless steels, which differs markedly from that of conventional carbon steels [10]. The most significant difference lies in the shape of the stress–strain curve. Stainless steel displays a nonlinear behavior from the onset of loading and significant strain hardening [12,13]. Therefore, the existing design methods are limited in their direct use for stainless steel because they are mainly designed for carbon steel.

In addition, Kamal et al. [8] carried out experimental investigations on stainless steel cellular beams. This study aimed to assess the flexural strength of cellular beams, which was observed to be 16.77% lower than that of plain-webbed beams, demonstrating the effect of opening geometry on structural efficiency. Li et al. [14] analyzed the influence of various opening shapes on the behavior of stainless steel beams. Their study revealed that elongated openings lead to the greatest reduction in resistance, thus emphasizing the shortcomings of current design rules for perforated stainless steel beams. In a recent investigation, Jiang et al. [15] carried out a numerical study on the patch loading resistance of stainless steel cellular beams. Using 2128 finite element simulations, new semi-empirical design equations were developed. More recently, Shamass and Guarracino [10] investigated the web-post buckling of high-strength and normal-strength steel cellular beams. They proposed a strut model whose geometric characteristics, namely length, width and inclination, are adapted to the beam geometry. Collectively, these studies have established the foundation of current design approaches for perforated steel beams.

While numerous studies have addressed the structural behavior of stainless steel members, the web-post buckling response of cellular beams fabricated from this material has yet to be thoroughly examined. Among the few theoretical studies currently available in the literature, the analytical framework put forward by Shamass and Guarracino [16] constitutes a noteworthy contribution. However, the authors highlighted the strong sensitivity of their model to the value of the tangent modulus E_t, and emphasized the need for further investigations to refine the value of the coefficient C_2. Accordingly, this study aims to propose a recalibration of C_2 for the austenitic stainless steel grades 1.4301, 1.4435, and 1.4541, as well as the ferritic grades 1.4016 and 1.4509, based on a new database comprising 1400 finite element simulations.

Throughout this study, several comparisons have been carried out. They are based on standards and analytical formulations that are representative in the field of stainless steel structures. First, the EN 1993-1-4 [17] standard was used as a reference for the design of stainless steel structures. It incorporates the specificities of the nonlinear behavior of stainless steel, which distinguishes it from standards applicable to carbon steel. Second, from a theoretical perspective, the choice of the Shamass and Guarracino [16] model is explained by the fact that this approach was specifically developed for web-post buckling of stainless steel cellular beams. It is a formula that integrates both the tangent modulus E_t and the coefficient C_2, which allows for a thorough analysis of the effect of strain hardening on the post-buckling behavior. Finally, the two models of Panedpojaman et al. [6] and Grilo et al. [9] were selected as a comparison basis to highlight and better understand the difference between the behavior of stainless steels and that of carbon steels. This comparison framework allows the results obtained to be positioned with respect to current practices while justifying the relevance of recalibrating the coefficient C_2.

To perform the parametric study, a series of finite element models was generated using the ABAQUS 2020 software. In contrast to simplified web-post models, a full-beam model was adopted in order to accurately represent the actual boundary conditions and thus provide more reliable numerical predictions. The cellular beams were discretized using S4R

shell elements, following a mesh sensitivity study carried out to achieve a balance between computational performance and numerical accuracy. The numerical model developed in this study was validated using experimental tests conducted on cellular beams in carbon steel [9], since, to date, no experimental tests on cellular beams in stainless steel have been reported in the literature. The primary goal of this validation is to verify the structural kinematics, which depend primarily on geometry and elastic stability. Eurocode 3, Part 1-4 [17], recommends using the Rasmussen constitutive model to accurately describe the nonlinear material behavior of stainless steel. Although calibration of the C_2 coefficient can ensure consistency between this material law and the analytical model, it does not replace direct experimental validation. To this end, it is recommended that future experimental campaigns be conducted on stainless steel cellular beams to validate the proposed design approach.

Furthermore, the design of stainless steel cellular beams requires the C_2 coefficient to be recalibrated, as the analytical model's high sensitivity to the tangent modulus E_t constitutes a major limitation to its practical application. To address this gap, a number of numerical investigations and a recalibration of the C_2 coefficient for several families of stainless steel were carried out in this study. The results obtained provide a solid and reliable basis for the design of stainless steel cellular beams, thereby confirming the relevance of research on the recalibration of the C_2 coefficient for such structural elements.

2. Finite Element Modeling and Validation

To investigate the web-post buckling resistance of cellular beams, simplified single web-post models are frequently employed. Although these models are capable of accurately capturing the local web-post buckling mechanism, they suffer from important limitations, particularly regarding the representation of boundary conditions, which have a considerable impact on the predicted response. Moreover, a single web-post model cannot accurately reproduce the overall structural behavior of the beam.

To achieve a more realistic and comprehensive representation of the structural response, a finite element model of the complete cellular beam section, including the stiffeners, was explicitly built using ABAQUS. Unlike simplified models, this full-beam model takes into account the beam's entire geometry and accurately reproduces the boundary and loading conditions of the experimental setup. As shown in Figure 3, the cellular beams were modelled to replicate simply supported conditions. A displacement-controlled load was applied to the top flange. At both ends of the beam, the translations in the X and Y directions, as well as the rotation about the Z axis, were restrained ($U_x = U_y = UR_z = 0$). In addition, a lateral constraint ($U_z = 0$) was applied at midspan to prevent lateral torsional buckling of the beams.

The finite element model developed in ABAQUS has proven to be sufficiently robust and reliable to represent the behavior of steel cellular beams and to accurately predict the different failure mechanisms that may occur in the web-post region. A validation analysis was executed prior to the parametric study to ensure the accuracy and consistency of the numerical model.

The reliability of the finite element model was assessed through a comparison between its predictions and experimental results obtained from simply supported cellular beams under concentrated loading. The experimental campaigns conducted by Grilo et al. [9] and Tsavdaridis and D'Mello [3] were selected as reference cases, since they provide a robust basis for evaluating the predictive performance of the numerical strategy.

The S4R shell elements used in this study are based on reduced integration. For this element type, ABAQUS applies the hourglass control formulation by default, which is based on the total stiffness approach (HOURGLASS = STIFFNESS). The ABAQUS documentation

states that this approach is used to suppress artificial hourglass modes that affect the post-buckling response. A mesh refinement study was carried out in order to identify the coarsest mesh that still yields reliable results, thereby ensuring both accuracy and reasonable computational effort. An element size of 10 mm was adopted in this work, as it provides a satisfactory compromise between solution precision and numerical cost.

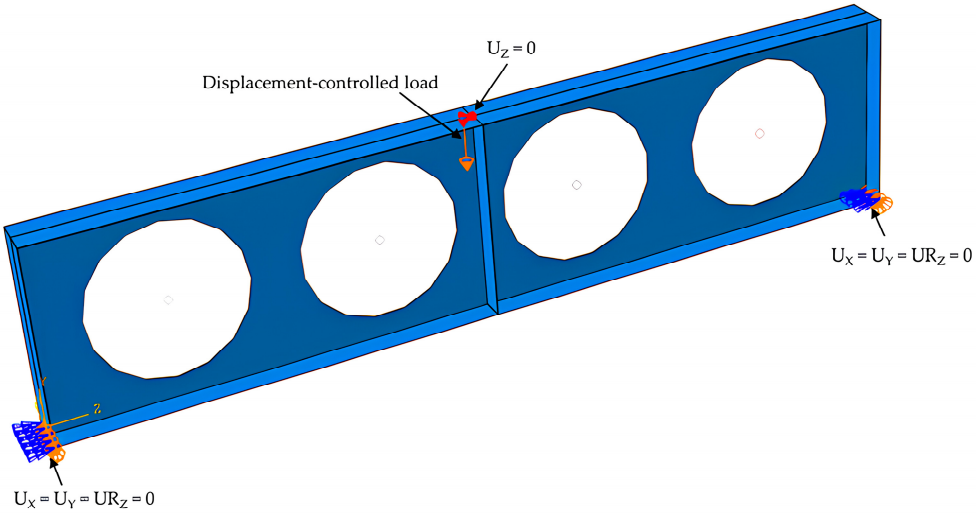


Figure 3. Geometry and applied boundary conditions for full beam.

The initial geometric imperfection was applied using the first buckling mode shape derived from the eigenvalue analysis, with an amplitude equal to H/500, consistent with recommendations from previous studies [4,14]. This choice is justified by established practice regarding cellular beams. Shamass et al. [18] conducted research on steel beams with elliptical openings. In these studies, the authors also used an imperfection value of dg/500. Their choice was justified by the fact that this value is suitable for steel beams with periodic web openings, due to the difficulty in estimating these geometric imperfections, which is primarily attributable to the manufacturing process. Furthermore, the choice of H/500 is also justified by the work conducted by Panedpojaman et al. [19], who used this imperfection amplitude for cellular beams. The imperfection amplitude H/500 used in this study is therefore consistent with previous work. A sensitivity analysis regarding geometric imperfections was performed. The simulations were repeated using three different imperfection amplitudes: H/1000, H/500, and H/250. The results show a 2% variation in the ultimate load over the range studied (relative to the reference value of H/500), confirming that the H/500 imperfection does not significantly affect the conclusions of this study.

Complex residual stress fields are generated in steel due to the manufacturing process of cellular beams. These stresses can reach up to 80% of the 0.2% proof stress in the case of austenitic stainless steels [20]. These residual stresses were not explicitly accounted for, as their effect on the overall buckling resistance of the web and flanges of thin-walled beams is generally considered less significant than that of geometric imperfections. Several previous studies conducted on stainless steel beams with similar geometric configurations support the decision not to include residual stresses. Indeed, their impact on the ultimate buckling resistance does not exceed 2% and is therefore often negligible [21]. Furthermore, other studies have demonstrated that incorporating geometric imperfections into a numerical model with a realistic nonlinear behavior law allows for the accurate reproduction of the combined influence of initial imperfections and residual stresses [22]. Recent research has shown that the use of geometric imperfection avoids explicit modeling of residual stresses [23]. In addition, work conducted by Silva et al. [24] on carbon steel cellular beams

under fire conditions has shown that, for the investigated cases, the load-bearing capacity and failure mode are not influenced by the presence or absence of residual stresses in the web.

To replicate the experimental setup of a simply supported beam, appropriate boundary conditions were defined. A vertical displacement was first applied incrementally to the upper flange, allowing the full structural response to be captured, including the post-buckling stage. Because lateral–torsional buckling fell outside the scope of this work, a lateral restraint was placed at mid-span in order to suppress global instability and promote the development of local failure mechanisms, in particular web-post buckling. Two stages were then adopted for the analysis. The first consisted of an eigenvalue analysis, which provided the buckling mode, the critical deformation shape and the critical load. The second was a nonlinear analysis, relying mainly on the Newton–Raphson method, designed to assess the real ultimate capacity of the beam. Geometric imperfections were incorporated so that buckling could be represented realistically.

Similar advanced numerical approaches have been applied to other steel components. For instance, new finite element studies have focused on helical anchors in clay [25,26] to accurately capture the nonlinearity of materials and failure mechanisms in steel structures using advanced numerical models. These studies demonstrate the fundamental role of finite element modeling in accurately predicting complex failure modes.

3. Numerical and Experimental Shear Buckling Loads: A Comparative Analysis

The finite element model established in this work was validated by directly comparing the numerical shear capacities (V_{FE}) with the experimental values (V_{test}), as reported in Figure 4. A close agreement is observed between the two sets of data. The mean value of the V_{FE}/V_{test} ratio is 1.04, with a standard deviation of 0.074 and a coefficient of variation of 7.12%. This low dispersion demonstrates the robustness of the numerical model across all tested configurations. For some data points, the slight dispersion observed is due to the simplified representation of welded joints and residual stresses in the numerical model, as well as to the inherent variability of experimental tests. However, the overall trend confirms the FE model's ability to predict the buckling resistance of web members. Such results validate the modeling approach adopted in this work and confirm its capacity to evaluate the web-post buckling resistance of stainless steel cellular beams with reasonable accuracy.

A key stage in the validation process is the comparison between the failure modes obtained from simulations and those presented in the literature. Several tests were conducted by Da Silva et al. [27] on steel cellular beams. These tests demonstrated that web-post buckling is the prevailing failure mode in cellular beams with closely spaced openings. Furthermore, Tsavdaridis and D'Mello [28] highlighted that the spacing and depth of the openings have a direct impact on the stability of the web-post. This web-post buckling phenomenon was observed for all the configurations studied. These observations agree with the experimental results presented by Grilo et al. [9], who also showed that web-post buckling is the dominant mechanism. Stainless steel is characterized by very pronounced work hardening, which delays the onset of buckling and significantly increases post-buckling strength. This behavior contrasts with that of carbon steel, where the yield plateau restricts stress redistribution. The Rasmussen constitutive law [13], used in this study, accurately captures this work hardening phenomenon. A satisfactory agreement is also observed between the numerical predictions and the experimental results, which shows that the model is capable of accurately reproducing the actual failure modes. The present observations validate the numerical approach used in the parametric study.

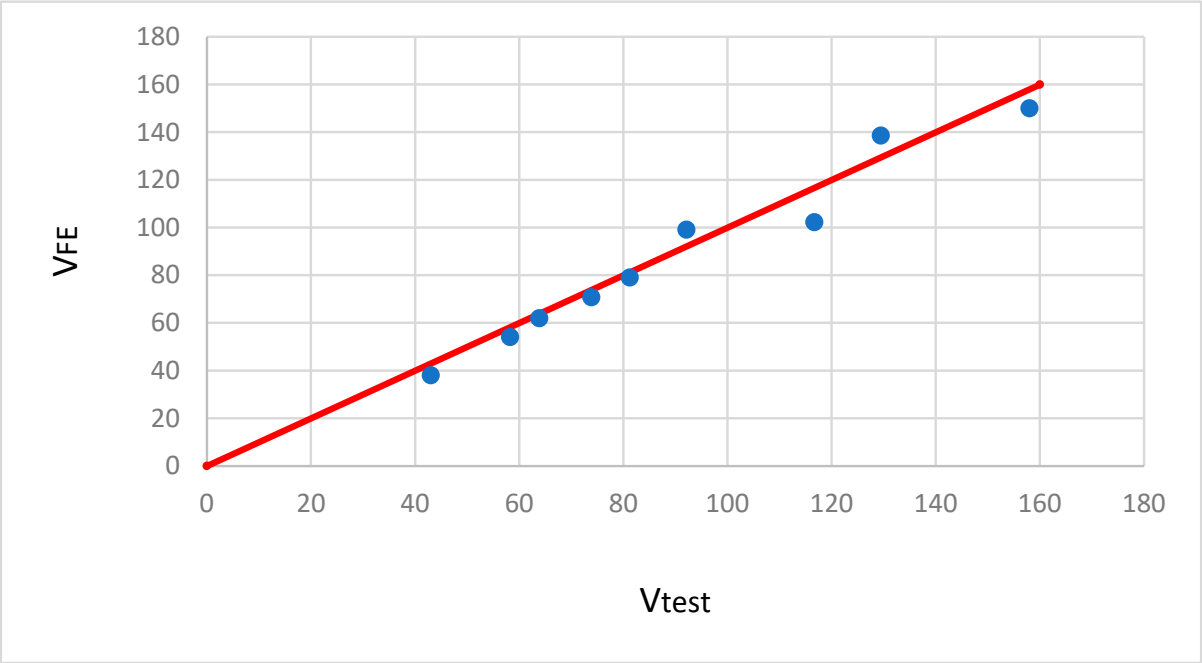


Figure 4. Numerical versus experimental shear buckling load: a comparative study.

4. Constitutive Modeling of Stainless Steel

For cellular beams, stainless steel tends to be selected primarily for its mechanical characteristics, such as strength, weldability and ductility, together with its resistance to corrosion. Within the field of civil engineering, five stainless steel families are commonly encountered: austenitic, ferritic, duplex, martensitic and precipitation-hardening grades [12,29]. This work focuses on austenitic and ferritic grades, which are characterized by their high ductility, good weldability and also excellent corrosion resistance [11,12]. It should be emphasized that stainless steel does not respond structurally in the same manner as carbon steel. Such a divergence stems primarily from the fact that the mechanical behavior of the two materials is not identical. The most evident contrast can be found in the profile of the stress–strain relationship. Carbon steel possesses a clearly identifiable yield point; beyond this threshold, the stress level remains practically unchanged while deformation grows substantially, and only a modest hardening phase precedes rupture. Stainless steel, by contrast, undergoes a progressive shift from elastic to plastic response, with no evident yield plateau and considerably greater isotropic hardening [12,30]. For stainless steel, the yield strength is typically defined by the 0.2% proof stress. Due to this particular stress–strain response, this material offers certain structural benefits, such as a marked capacity for stress redistribution through strain hardening and good toughness. The formulation proposed by Rasmussen [13] is the model adopted in this work to describe the mechanical response of stainless steels. This model is characterized by its ability to accurately reproduce the specific characteristics of stainless steel behavior, more precisely its non-linear stress–strain relationship, which differs significantly from that of carbon steel. Furthermore, several previous studies have validated the Rasmussen model, which has been widely used in the numerical analysis of steel structures, in particular beams [1,16] and columns [31]. In addition, Eurocode 3, Part 1–4 [17], recommends the adoption of Rasmussen's law for the modeling of stainless steel grades.

The constitutive model proposed by Rasmussen [13] is expressed through Equations (1) and (2):

$$\varepsilon = \frac{\sigma}{E} + 0.002\left(\frac{\sigma}{\sigma_{0.2}}\right)^{n} \text{ for } 0 \le \sigma \le \sigma_{0.2} \quad (1)$$

$$\varepsilon = \varepsilon_{0.2} + \frac{\sigma - \sigma_{0.2}}{E_2} + \varepsilon_{up}^{*}\left(\frac{\sigma - \sigma_{0.2}}{\sigma_u - \sigma_{0.2}}\right)^{m} \text{ for } \sigma_{0.2} \le \sigma \le \sigma_u \quad (2)$$

With:

$$\varepsilon_{up}^{*} = \varepsilon_u - \varepsilon_{0.2} - \frac{\sigma_u - \sigma_{0.2}}{E_2}$$

$$m = 1 + 3.5\frac{\sigma_{0.2}}{\sigma_u}$$

$$\varepsilon_u = \min\left(1 - \frac{\sigma_{0.2}}{\sigma_u}, A\right)$$

$$E_2 = \frac{E}{1 + 0.002\frac{n}{e}}$$

$$e = \frac{\sigma_{0.2}}{E}$$

where ε and σ denote the uniaxial strain and stress, respectively; ε_u is the ultimate tensile strain; $\varepsilon_{0.2}$ represents the 0.2% strain associated with $\sigma_{0.2}$; m and n are strain hardening coefficients; A is the stainless steel elongation and E_2 is the slope of the stress–strain curve at $\varepsilon_{0.2}$.

5. Parametric Study

The parametric investigation aims to identify and quantify the effect of material and geometric variables on the critical shear buckling load of stainless steel cellular beams. By identifying the most unfavorable configurations, this analysis seeks to provide a basis for enhancing current design procedures.

The geometry of the web-posts is characterized by the following parameters [5]:

$$e = \frac{d_0}{2} - \sqrt{\left(\frac{d_0}{2}\right)^2 - \left(\frac{s - d_0}{2}\right)^2} \quad (3)$$

$$H = d + \frac{d_0}{2} - e \quad (4)$$

$$s_0 = s - d_0 \quad (5)$$

Figure 5 presents the boundary conditions assigned to the isolated web model. On the left side of the model, translational displacements were constrained ($U_x = U_y = U_z = 0$) to ensure the kinematic stability of the model and to reproduce the connection conditions associated with T-sections. On the right side of the web, displacement along the X axis and rotations about the X and Y axes were restrained ($U_x = UR_x = UR_y = 0$). At the top and bottom ends of the right side, displacement along the X axis and rotations about the Y and Z axes were blocked ($U_x = UR_y = UR_z = 0$) to limit unwanted movement. Finally, a vertical shear load was applied to the right side of the model.

The parametric investigation was conducted by systematically varying all geometric and material factors likely to influence the buckling response of the web member. An overview of the selected parameters, together with their respective variation intervals, is provided in Table 1. The study covers five austenitic stainless steel grades and two ferritic grades. Their mechanical characteristics are listed in Table 2.

The combination of all these parameters led to the generation of 1400 numerical configurations. Each configuration was analyzed using the finite element method to determine the critical shear buckling load V_{FE}.

Figure 6 shows the distribution of von Mises stresses for a representative configuration. Buckling initiates at the web member, where the stresses are clearly concentrated, while the flanges remain under less stress. This confirms that web-post buckling (WPB) is the dominant failure mode for the investigated configurations.

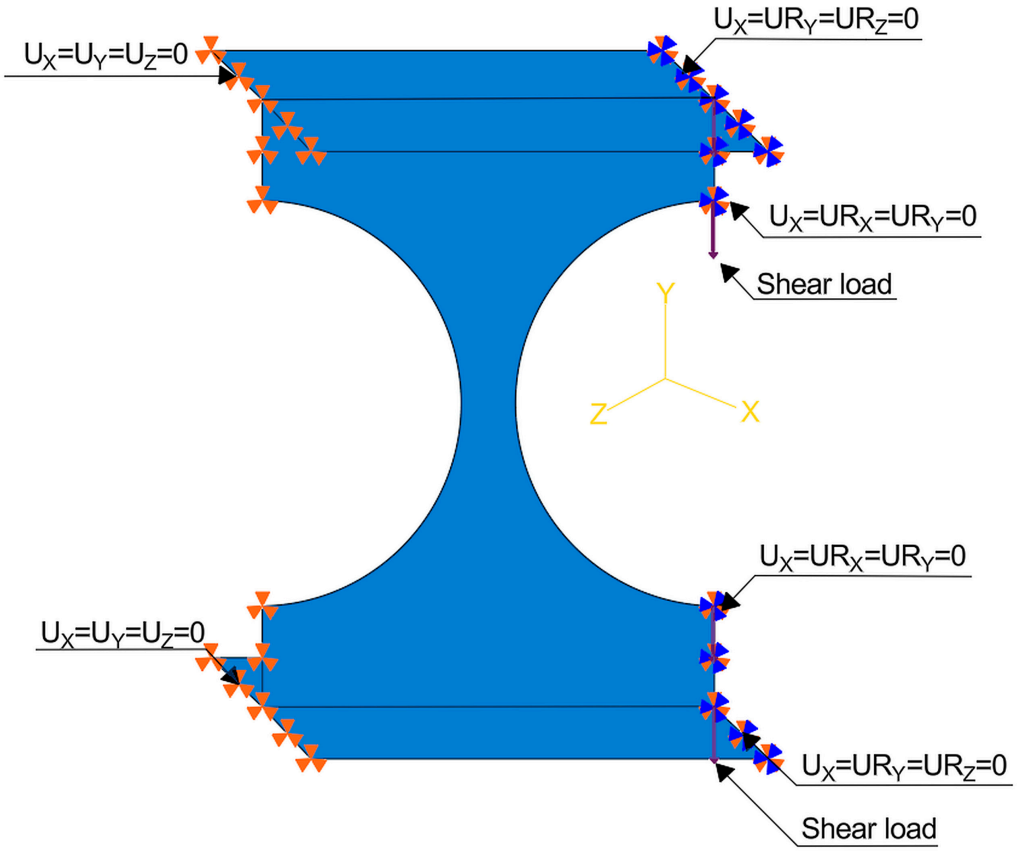


Figure 5. Geometry and applied boundary conditions for a single web-post.

Table 1. Summary of the parametric study.

Parameter	Symbol	Range	Increment
Opening spacing ratio	s/d_o	1.1–1.4	0.1
Web slenderness ratio	d_o/t_w	33.07–49.60	Variable
Opening ratio	d_o/d	0.8–1.2	0.1
Young's modulus	E (MPa)	183,611–206,880	Variable
Yield strength	$\sigma_{0.2}$ (MPa)	266–331	—

Table 2. Mechanical properties of stainless steels.

Stainless Steel Type	Grade	E (Gpa)	$\sigma_{0.2\%}$ (N/mm^2)	σ_u (N/mm^2)
Austenitic	1.4301	199.512	266	595.54
	1.4435	186.718	322	620.38
	1.4435	189.126	322	625.27
	1.4541	192.915	272	590.23
	1.4541	183.611	271	572.88
Ferritic	1.4016	195.781	311	450.51
	1.4509	206.880	331	478.33

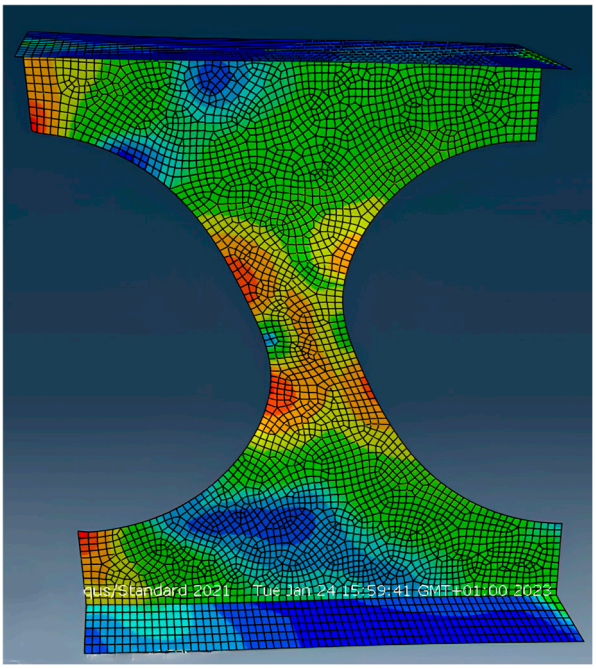
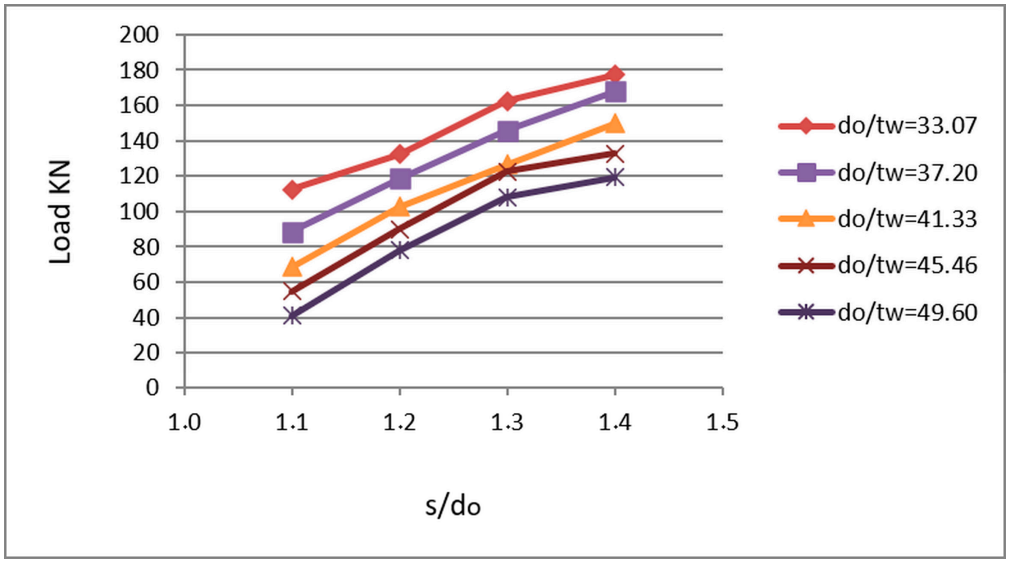


Figure 6. Web-post buckling failure mode (Max: $+5.131 \times 10^2$).

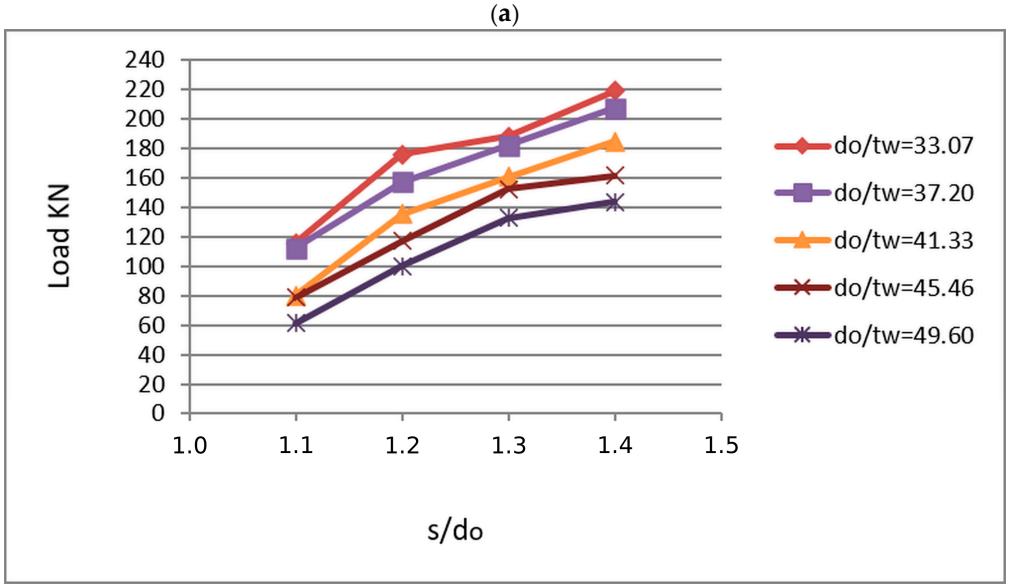
6. Effects of s/d_o and d_o/t_w Ratios and Stainless Steel Grade

This section investigates the influence of the s/d_o and d_o/t_w ratios. These geometric parameters lead to changes in the shear load due to the buckling of austenitic and ferritic stainless steel members. In particular, the study is limited to the austenitic grades 1.4301, 1.4435 and 1.4541 and the ferritic grades 1.4016 and 1.4509. Figure 7 shows the variation in buckling shear load for stainless steel cellular beams for different d_o/t_w values: 33.07, 37.20, 41.33, 45.46 and 49.60. In all cases a clear trend of increasing critical shear load with increasing s/d_o is observed. This behavior is explained by a geometric stiffening effect. As the openings are spaced further apart, the beam becomes more resistant to web–post buckling. In contrast, higher buckling shear loads are also achieved by decreasing the d_o/t_w ratio. This indicates that larger openings reduce the web rigidity, thereby making the beam more prone to buckling.

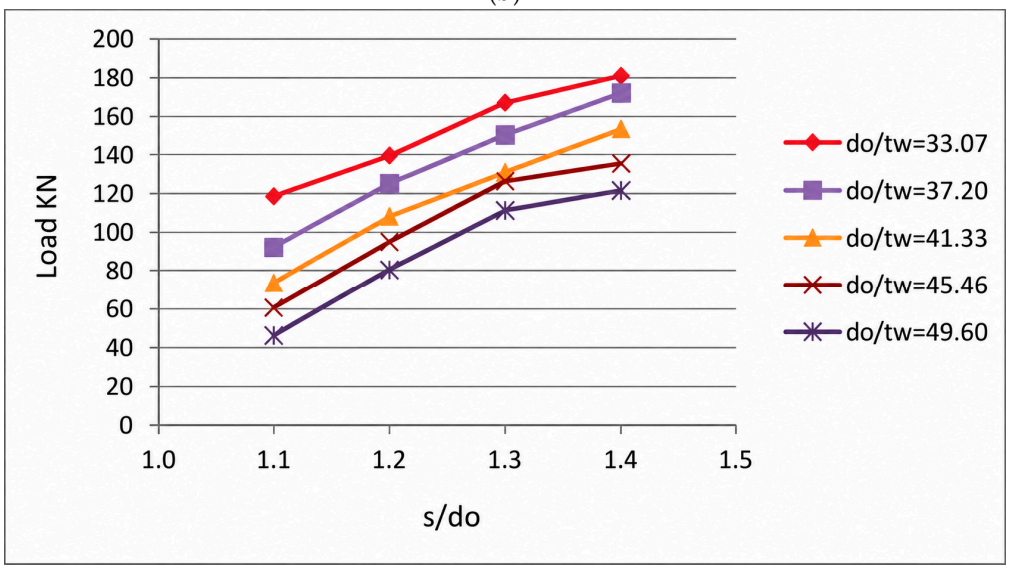
An analysis of variance was performed on all the numerical results to determine the significance of the parameters on buckling resistance. This approach partitions the variability in the normalized resistance in order to identify the major factors affecting the performance of the beams. The results show that the s/d_o parameter is the most influential factor, accounting for 46.44% of the total variance in the normalized resistance. Subsequently, the slenderness ratio d_o/t_w accounts for 35.92%. By contrast, the grade of stainless steel has a limited impact, accounting for 8.89%. These percentages indicate, on the one hand, that the spacing of the openings has a predominant impact on the buckling resistance of the web members of stainless steel cellular beams. This is because the stiffness, which is directly determined by the width of the web, depends mainly on the distance between the openings. On the other hand, the geometric configuration of the beam appears to exert a more pronounced effect on the buckling response than the mechanical characteristics of the material.



(**a**)

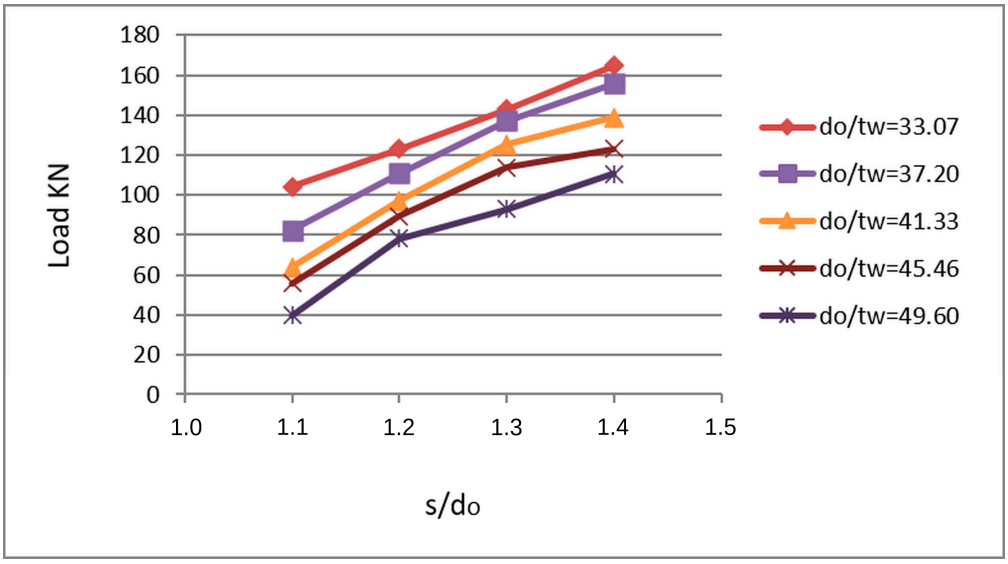


(**b**)

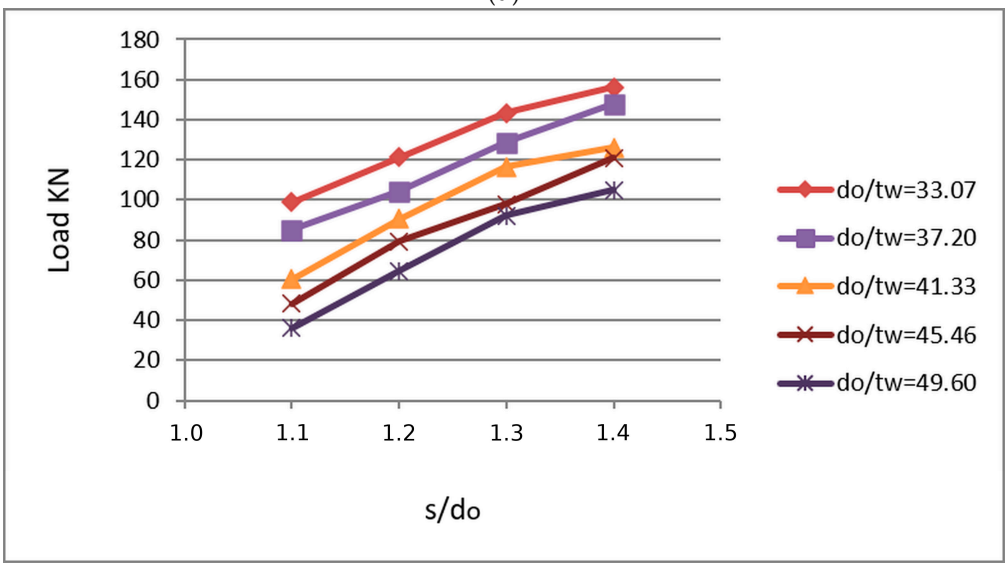


(**c**)

Figure 7. *Cont.*



(**d**)



(**e**)

Figure 7. Effect of s/d_o and d_o/t_w on the shear buckling resistance of stainless steel cellular beams: (**a**) austenitic 1.4301; (**b**) austenitic 1.4435; (**c**) austenitic 1.4541; (**d**) ferritic 1.4509; (**e**) ferritic 1.4016.

The results show that the buckling resistance is governed by the nonlinear behavior of the material. This dependence differs from one grade to another, which is mainly due to the specific properties of each stainless steel family.

The austenitic grades considered, namely 1.4301, 1.4435 and 1.4541, are characterized by pronounced strain hardening, which results in an improvement of the post-buckling resistance. Indeed, their high ductility and significant work hardening enhance the load-bearing capacity through stress redistribution within the web-post. In contrast, ferritic stainless steels (1.4016 and 1.4509) exhibit more limited ductility compared to austenitic steels and less pronounced strain hardening. These characteristics lead to a lower post-buckling resistance. The results show that for identical geometries, the resistance of austenitic steels is higher than that of ferritic steels.

This difference in nonlinear behavior between these families of stainless steels highlights the importance of recalibrating the C_2 coefficient for each of these families. This recalibration is a crucial step that enables the specific response of each family of stainless

steels to be accurately represented, thanks to its ability to incorporate the actual influence of work hardening into the model.

7. Analytical Prediction of Web-Post Buckling Resistance in Stainless Steel Cellular Beams

In order to predict the web-post buckling, Shamass and Guarracino [10] put forward a theoretical model characterized by its ability to consider the main parameters influencing the strut's response, namely its geometric characteristics, the mechanical properties of the material and the support conditions. The main objective of this approach is to describe the actual behavior of the structure realistically. The formulation relies on the classical strut analogy, where the portion of the web located between two adjacent openings is assimilated to an equivalent diagonal member subjected to axial compression. This model is distinguished by the introduction of the parameter E_t (tangent modulus) and the coefficient C_2, which allow the nonlinear behavior of stainless steel to be taken into account.

The equations shown below are used to calculate the critical shear-buckling load V of stainless steel cellular beams. They include the calculation of the width of the web, b, its inclination, α', its buckling length, l_0', the critical load, Q_c, the boundary condition coefficient, β, the tangent modulus, E_t, and finally the shear strength, V, which are calculated using Equations (6), (7), (9), (10), (11), (12) and (13), respectively:

$$b = \frac{[H(d_0 + s_0) - \frac{\pi}{4}d_0^2]}{\gamma H} \tag{6}$$

With: $\gamma = 6$

$$\alpha' = \sin^{-1}\left(\frac{R + \frac{b}{2}}{\sqrt{\frac{b^2}{4} + Rs_0 + \frac{s_0^2}{4}}}\cos\alpha\right) \tag{7}$$

where

$$\alpha = \sin^{-1}\frac{R}{R + \frac{s_0}{2}} \tag{8}$$

With: $R = \frac{d_0}{2}$

$$l_0' = \frac{H + d_0}{2}\frac{1}{\sin\alpha'} \tag{9}$$

$$Q_c = \frac{n^2\pi^2 E_t b t_w^2}{12(\beta l_0')^2} \tag{10}$$

The value $n = 2$ is adopted to reflect the two-wave deformation pattern characteristic of web-post buckling, a failure mode that was systematically observed throughout both the numerical simulations and the experimental tests. In this expression, E_t stands for the tangent modulus of the material, evaluated at the critical buckling stress level.

$$\beta = k\frac{t_w}{H} \tag{11}$$

$$E_t = \frac{\sigma_u - \sigma_{0.2}}{C_2\varepsilon_u - \varepsilon_y} \tag{12}$$

The shear-buckling load:

$$V = 2\frac{Q_c}{s}(H - t_f)\cos\alpha' \tag{13}$$

8. Recalibration of the C_2 Coefficient in the Strut Model for Stainless Steels

In the connecting rod model proposed by Shamass and Guarracino [10], the tangent modulus E_t is calculated using the following Equation (12) [32]:

$$E_t = \frac{\sigma_u - \sigma_{0.2}}{C_2\varepsilon_u - \varepsilon_y}$$

The C_2 coefficient is a calibration factor whose purpose is to adjust the E_t parameter to account for the non-linear behavior of stainless steel. This coefficient has a direct effect on the stiffness of the compressed strut; therefore, it affects the shear resistance. This parameter depends on the specific grade of stainless steel in question. Shamass and Guarracino [16] propose a value of $C_2 = 0.023$ for austenitic stainless steel and a value of $C_2 = 0.015$ for ferritic stainless steel. However, these authors themselves have highlighted a major limitation of their model: the results are highly sensitive to the value of the tangent modulus E_t, and therefore to C_2. They explicitly called for further investigations to refine this parameter and improve the reliability of their model. To this end, this study proposes a recalibration of C_2 specifically for the austenitic stainless steel grades 1.4301, 1.4435 and 1.4541, and for the ferritic stainless steel grades 1.4016 and 1.4509.

These results confirm that the single value $C_2 = 0.023$ proposed by Shamass and Guarracino [16] (Figure 8) is not optimal for all austenitic grades. A calibration specific to each grade is therefore recommended (Figure 9).

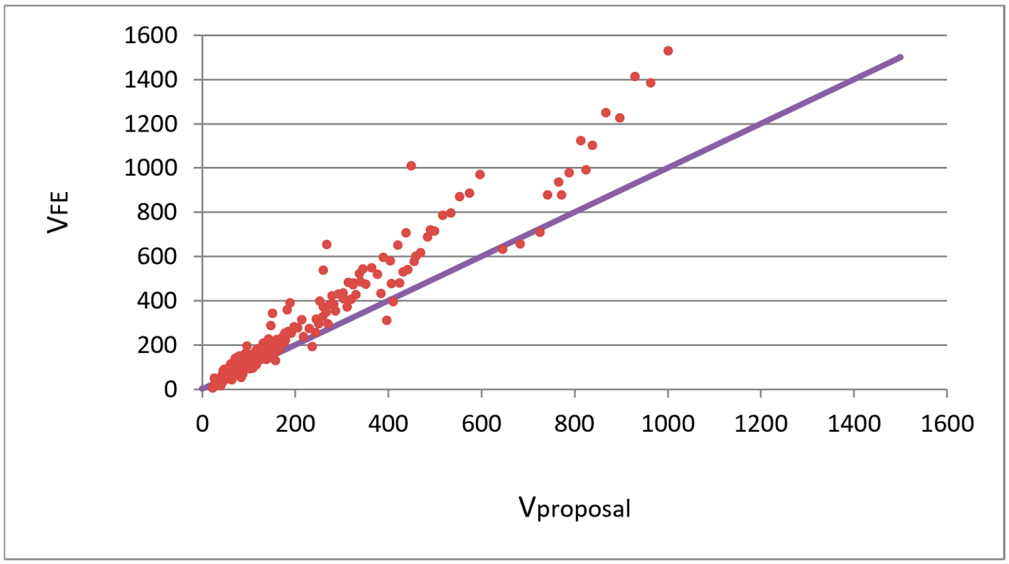


Figure 8. Austenitic stainless steel 1.4435 (E = 186,718 MPa)—before recalibration.

Furthermore, in the case of ferritic stainless steels, no recalibration was carried out; the value of the C_2 parameter used is that proposed by Shamass and Guarracino [16] ($C_2 = 0.015$). Figure 10 shows a comparison between the numerically obtained V_{FE} values and the values provided by the $V_{proposal}$ model; the data points demonstrate an excellent correlation between the predicted values and the results calculated using the finite element method.

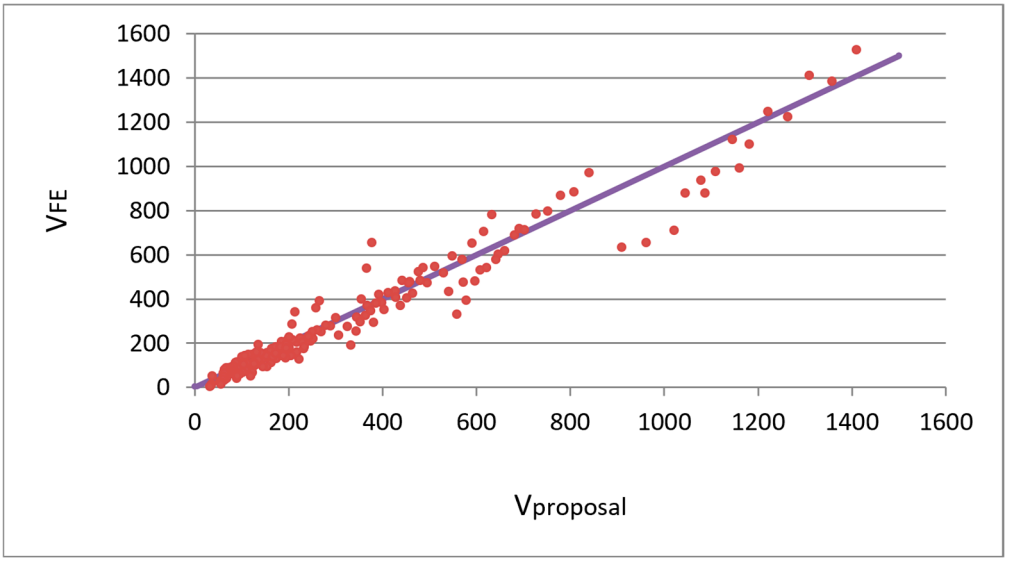


Figure 9. Austenitic stainless steel 1.4435 (E = 186,718 MPa)—after recalibration.

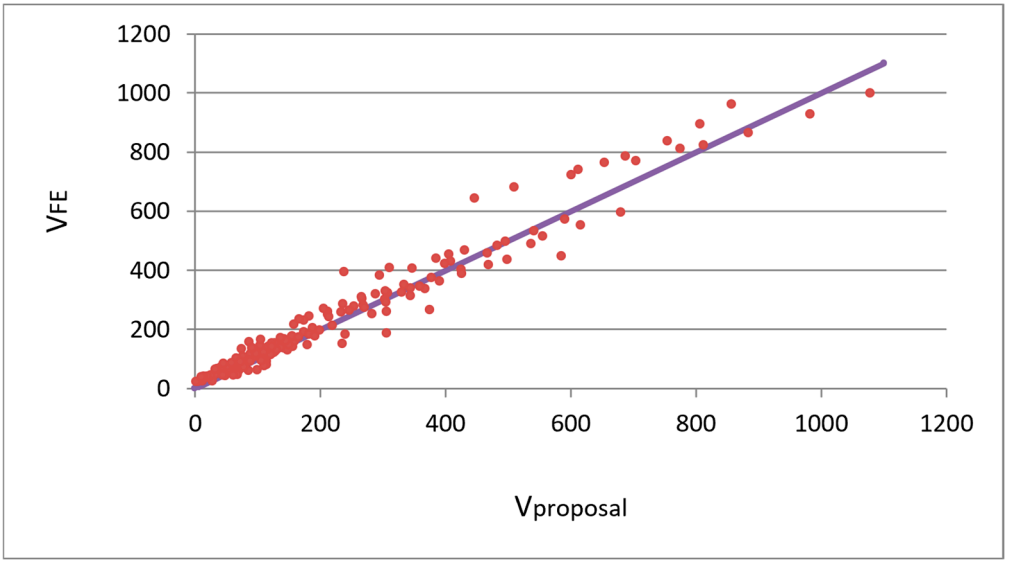


Figure 10. Ferritic stainless steel 1.4016 (E = 195,781 MPa)—without recalibration.

9. Results and Discussion

One of the main parameters in the connecting rod model proposed by Shamass and Guarracino [16] is the coefficient C_2. This coefficient is used in the calculation of the tangent modulus and directly affects the stiffness of the equivalent strut, thereby significantly influencing the buckling resistance of the web struts. To this end, and to ensure the reliability of the model, particularly for new grades of stainless steel such as those examined in this study, a precise calibration of C_2 is essential. The objective of this analysis is to assess the model's sensitivity to the C_2 coefficient, so as to subsequently identify the optimal value of C_2 that delivers the best performance for the various grades studied. In this study, the recalibrated values of the coefficient C_2 are not arbitrary but result from a systematic optimization procedure. This recalibration aims to minimize, as much as possible, the discrepancy between the values obtained from the Shamass and Guarracino [16] model and the numerical results generated by the finite element method.

Firstly, the geometric parameters as well as the mechanical properties of each configuration were fixed. Then, for each value of C_2, the tangent modulus E_t and the resistance, $V_{proposal}$ were calculated for each configuration. Subsequently, using the Excel Solver tool, the value of C_2 was varied until the value for which the mean relative error is minimal was obtained.

To evaluate the reliability and the robustness of the model, a sensitivity analysis was performed around the optimal value. This procedure, which was applied separately to the austenitic and ferritic stainless steel grades, highlighted the importance of calibration according to the steel family and grade.

The recalibrated values of C_2 for each grade of stainless steel are summarized in Table 3. The C_2 coefficient is used to adjust the slope of the stress–strain curve in the plastic range so that it matches the finite element results. As plastic strain increases, the tangent modulus E_t gradually decreases due to strain hardening. This behavior is calibrated by the C_2 coefficient for each steel grade. The distinct values of the C_2 coefficient obtained are related to slight differences in the stress–strain curves. These differences can be explained by variations in material parameters for each steel grade. To ensure the accuracy of the analytical model, it is necessary to adjust a specific C_2 value for each steel grade.

Table 3. The recalibrated values of C_2 for each grade of stainless steel.

Stainless Steel Type	Grade	E (Gpa)	C_2
Austenitic	1.4301	199.512	0.021
	1.4435	186.718	0.019
	1.4435	189.126	0.019
	1.4541	192.915	0.020
	1.4541	183.611	0.020
Ferritic	1.4016	195.781	0.015
	1.4509	206.880	0.015

Figure 8 presents a comparison between the strengths predicted using the Shamass and Guarracino [16] model and those obtained numerically using V_{FE}. For austenitic stainless steels of grades 1.4301, 1.4435 and 1.4541, the values obtained using the coefficient $C_2 = 0.023$ underestimate the web buckling resistance with a $V_{FE}/V_{proposal(C2=0.023)}$ ratio of 1.18. However, the values obtained by recalibrating C_2 are significantly closer to the values obtained numerically. The recalibrated model is characterized by excellent average accuracy ($V_{FE}/V_{proposal} = 0.98$), good predictive power ($R^2 = 0.878$), and a standard deviation of 0.14. This dispersion is acceptable for this type of simplified model. It is primarily due to the simplifications inherent in the strut model, particularly for configurations with large openings. The obtained coefficient of determination shows that the model explains 87.8% of the variability of the web-post buckling resistance. The remaining 12.2% are due to several factors, namely the scatter in the numerical simulations and the simplifications of the analytical model. The scatter plot shown in Figure 11 reveals that the majority of the data points are distributed around the diagonal line. However, there is a slight tendency for the analytical model to overestimate capacity for certain specific configurations. This indicates that the calibration process does not introduce a severe systematic error, but rather a slight conservative tendency, which is generally acceptable for design purposes. This behavior is consistent with the results obtained by Shamass and Guarracino [16].

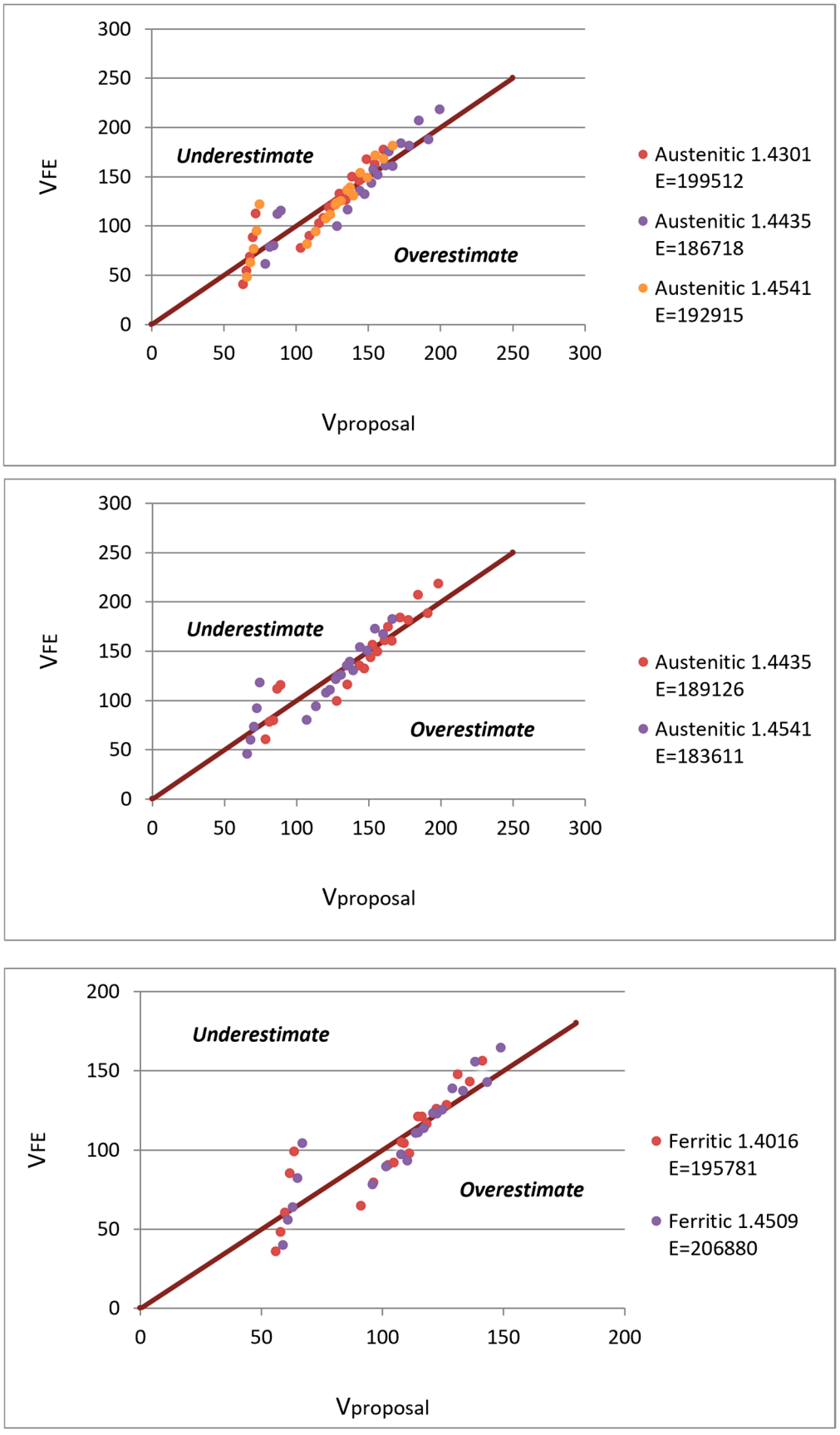


Figure 11. Comparison of analytical and numerical shear buckling loads for all stainless steel grades.

Recalibrating the C_2 parameter significantly improves the model's predictive performance. This recalibration has reduced the gap between the predicted values and the numerical results. These results confirm that recalibrating parameter C_2 is an essential step in adapting the model proposed by Shamass and Guarracino [16] to the specific characteristics of austenitic stainless steel grades 1.4301, 1.4435 and 1.4541.

The error related to the simplification introduced by the equivalent strut model is compensated in this study by calibrating the C_2 coefficient on the basis of 1400 finite-element models that account for the combined effects of the loads. This simplification still leads to a good correlation ($R^2 = 0.878$), suggesting that the model can satisfactorily reproduce the actual behavior.

Unlike austenitic stainless steel, in the case of the ferritic stainless steel family specifically grades 1.4016 and 1.4509, the coefficient $C_2 = 0.015$ proposed by Shamass and Guarracino [16] has yielded an accurate estimate of the buckling resistance of the web members in cellular beams. The ratio $V_{FE}/V_{proposal} = 0.95$ confirms that the value of the coefficient $C_2 = 0.015$ requires no recalibration for these grades. This model, with a value of $C_2 = 0.015$, predicts the buckling resistance of the web members of ferritic stainless steel cellular beams with a high degree of accuracy.

The results clearly show that the analytical model is characterized by high predictive accuracy. Good agreement is observed for all five different types of stainless steel, despite their differing yield strengths and work-hardening limits. The new, recalibrated C_2 values provide engineers with a more accurate tool for predicting the buckling resistance of the web members in stainless steel cellular beams (Figure 11). This recalibration contributes to safer and more efficient design of stainless steel structures.

In the context of the present study, the numerical model developed has certain limitations, although it is likely to yield meaningful results. First, this model has been validated only by comparison with tests carried out on carbon steel cellular beams; this is mainly due to the lack of experimental tests on stainless steel cellular beams. Consequently, experimental tests are required to confirm the numerical results. Furthermore, this parametric study was carried out over a limited geometric domain. The results obtained in this study are valid only within the range of parameters considered. Outside these limits, new failure modes may develop. According to studies conducted by Panedpojaman et al. [6], the depth of the T-section is the key parameter that distinguishes web-post buckling from Vierendeel bending. Tsavdaridis and Galiatsatos [33] also showed that, when the sections are very close together, the Vierendeel shear failure mode occurs, whereas, as the spacing increases, out-of-plane buckling becomes the predominant failure mode. When the spacings are larger ($s/d_o > 1.4$), the buckling resistance of the web members increases; however, other failure modes—namely global bending or lateral-torsional buckling—can occur when the beam is not laterally restrained. For more slender webs ($d_o/t_w > 50$), WPB remains the primary failure mode, but lateral-torsional buckling may develop in the absence of lateral restraint. Further studies are needed to generalize the proposed model to these configurations.

10. Conclusions

This study aimed to recalibrate the C_2 coefficient of the strut model proposed by Shamass and Guarracino for stainless steel cellular beams. This calibration is based on a numerical parametric study covering seven grades of stainless steel (five austenitic: 1.4301, 1.4435 (with two distinct Young's modulus values), and 1.4541 (also with two different Young's modulus values) and two ferritic grades: 1.4016 and 1.4509) and two hundred geometric configurations (s/d_o ranging from 1.1 to 1.4 and d_o/t_w ranging from 33.07 to 49.60).

The strut model proposed by Shamass and Guarracino is a robust and accurate tool for predicting the buckling of web members in stainless steel cellular beams. Nevertheless, the study highlights the importance of recalibrating the C_2 coefficient to improve the model's reliability and performance. For austenitic stainless steels, the new C_2 values (0.021 for 1.4301, 0.019 for 1.4435, and 0.020 for 1.4541) proposed for the three grades significantly improve the model's accuracy. In contrast, for ferritic stainless steels, the study confirms that the model remains applicable with $C_2 = 0.015$ without further recalibration.

The results show that the model's accuracy depends heavily on the specific steel grade. Therefore, it is necessary to recalibrate the C_2 coefficient for each family of stainless steel in order to reliably predict the buckling resistance of the web members.

Although the proposed approach proves to be an effective and reliable tool for the design of stainless steel cellular beams, the lack of experimental tests on stainless steel cellular beams represents a limitation of this study. Future work should focus on the experimental validation of the model and the extension of the calibration to other grades of stainless steel, in order to generalize the proposed design approach.

Author Contributions: Conceptualization, I.B., O.M. and R.S.; methodology, I.B.; software, I.B.; validation, I.B.; investigation, I.B.; data curation, I.B.; writing—original draft, I.B., O.M. and R.S.; writing—review & editing, I.B., O.M. and R.S.; supervision, O.M. and R.S.; project administration, O.M. All authors have read and agreed to the published version of the manuscript.

Funding: This research received no external funding.

Data Availability Statement: The data presented in this study are available from the corresponding author on reasonable request.

Conflicts of Interest: The authors declare no conflict of interest.

References

1. Cashell, K.A.; Malaska, M.; Khan, M.; Alanen, M.; Mela, K. Experimental and numerical analysis of stainless steel cellular beams in fire. *Fire Saf. J.* **2021**, *121*, 103277. [CrossRef]
2. Sheehan, T.; Dai, X.; Lam, D.; Aggelopoulos, E.; Lawson, M.; Obiala, R. Experimental study on long spanning composite cellular beam under flexure and shear. *J. Constr. Steel Res.* **2016**, *116*, 40–54. [CrossRef]
3. Tsavdaridis, K.D.; D'Mello, C. Web buckling study of the behaviour and strength of perforated steel beams with different novel web opening shapes. *J. Constr. Steel Res.* **2011**, *67*, 1605–1620. [CrossRef]
4. Namba, J.Y.; Ribeiro, I.E.d.S.; Tavares, H.C.A.; Rossi, A.; Krahl, P.A.; Torres, C.A.B.; Martins, C.H. Evaluation of web post-buckling in high-strength cellular steel and high-strength concrete composite beams: A numerical study. *Eng. Struct.* **2025**, *334*, 120223. [CrossRef]
5. Ward, J.K. *Design of Composite and Non-Composite Cellular Beams*; SCI Publication 100; The Steel Construction Institute: Berkshire, UK, 1990.
6. Panedpojaman, P.; Thepchatri, T.; Limkatanyu, S. Novel design equations for shear strength of local web-post buckling in cellular beams. *Thin-Walled Struct.* **2014**, *76*, 92–104. [CrossRef]
7. Erdal, F.; Saka, M.P. Ultimate load carrying capacity of optimally designed steel cellular beams. *J. Constr. Steel Res.* **2013**, *80*, 355–368. [CrossRef]
8. Kamal, A.I.A.; Zakwan, F.A.A.; Ismail, R. Flexural behavior of cellular stainless-steel beams: Experimental and statistical analysis. *Asian J. Civ. Eng.* **2025**, *26*, 2303–2317. [CrossRef]
9. Grilo, L.F.; Fakury, R.H.; de Castro e Silva, A.L.R.; Veríssimo, G.d.S. Design procedure for the web-post buckling of steel cellular beams. *J. Constr. Steel Res.* **2018**, *148*, 525–541. [CrossRef]
10. Shamass, R.; Guarracino, F. Numerical and analytical analyses of high-strength steel cellular beams: A discerning approach. *J. Constr. Steel Res.* **2020**, *166*, 105911. [CrossRef]
11. Rossi, B. Discussion on the use of stainless steel in constructions in view of sustainability. *Thin-Walled Struct.* **2014**, *83*, 182–189. [CrossRef]
12. Gardner, L. The use of stainless steel in structures. *Prog. Struct. Eng. Mater.* **2005**, *7*, 45–55. [CrossRef]
13. Rasmussen, K.J.R. Full-range stress–strain curves for stainless steel alloys. *J. Constr. Steel Res.* **2003**, *59*, 47–61. [CrossRef]

14. Wang, Y.; Chen, B.; Wang, W.; Ye, Q.; Liu, J.-Z.; Li, B.; Wang, Z. Experimental and numerical study of stainless steel beams with different opening shapes in the marine environment. *Ocean Eng.* **2025**, *342*, 123218. [CrossRef]
15. Jiang, Y.; Li, L.; Zhu, L.; Xu, W.; Wang, Y.; Chen, B.; Chi, Y.; Wu, G. Design provision assessment for localized-loading resistance of welded stainless steel I-beams with web openings. *Case Stud. Constr. Mater.* **2025**, *22*, e04854. [CrossRef]
16. Shamass, R.; Guarracino, F. Numerical and Theoretical Modelling of the Web-Post Buckling of Stainless Steel Cellular Beams. *CE/Papers* **2021**, *4*, 1551–1557. [CrossRef]
17. *EN 1993-1-4*; Eurocode 3: Design of Steel Structures—Part 1–4: General Rules—Supplementary Rules for Stainless Steels. CEN: Brussels, Belgium, 2006.
18. Shamass, R.; Ferreira, F.P.V.; Limbachiya, V.; Santos, L.F.P.; Tsavdaridis, K.D. Web-post buckling prediction resistance of steel beams with elliptically-based web openings using Artificial Neural Networks (ANN). *Thin-Walled Struct.* **2022**, *180*, 109959. [CrossRef]
19. Panedpojaman, P.; Sae-Long, W.; Yapa, R.; Chaiviriyawong, P. Design of Cellular Members under Axial-Shear-Flexure Interaction. *J. Appl. Comput. Mech.* **2024**, *10*, 754–769. [CrossRef]
20. Yuan, H.X.; Wang, Y.Q.; Shi, Y.J.; Gardner, L. Residual stress distributions in welded stainless steel sections. *Thin-Walled Struct.* **2014**, *79*, 38–51. [CrossRef]
21. Reis, A.; Lopes, N.; Real, E.; Vila Real, P. Stainless Steel Plate Girders Subjected to Shear Buckling at Normal and Elevated Temperatures. *Fire Technol.* **2017**, *53*, 815–843. [CrossRef]
22. Amani, M.; Al-Emrani, M.; Khalili, S. Imperfection Sensitivity of Plastic Shear Buckling Behavior in Corrugated Web Stainless Steel beams. *CE/Papers* **2023**, *6*, 1793–1798. [CrossRef]
23. Pazin, V.A.; Tsavdaridis, K.D.; Ferreira, F.P.V.; De Nardin, S. Residual stresses and geometric imperfections in high-strength steel cellular beams: Sensitivity analysis. *J. Constr. Steel Res.* **2026**, *236*, 110017. [CrossRef]
24. Silva, J.; Dalcanal, P.; Mesquita, L. Numerical Analysis of Cellular Steel Beams Failure Modes in Fire Conditions. In *Proceedings of the Advances in Fire Safety Engineering*; Piloto, P.A.G., Rodrigues, J.P., Silva, V.P., Eds.; Springer International Publishing: Cham, Switzerland, 2020; pp. 78–92.
25. Wang, L.; Zhang, L.; Chen, H.; Zhang, T.; Yi, J.; Zhang, J.; Zhou, T.; Chen, L.; Xu, Y.; Tian, Y.; et al. Combined effects of anchor geometry and soil spatial variability on the probabilistic pullout capacity of helical anchors. *Comput. Geotech.* **2026**, *200*, 108482. [CrossRef]
26. Zhang, T.; Wang, L.; Chen, L.; Lu, W.; Hao, D.; Shao, W.; Zhang, C.; Tian, Y. Numerical analysis of post-cyclic ultimate bearing capacity of helical anchors in clay. *Ocean Eng.* **2026**, *352*, 124583. [CrossRef]
27. da Silva, L.V.; Giacomitti, N.; Ferreira, D.; Lopes, N.; Mesquita, L.M.R. Experimental investigation of cellular steel beams at ambient and elevated temperatures. *Fire Saf. J.* **2026**, *159*, 104574. [CrossRef]
28. Tsavdaridis, K.D.; D'Mello, C. Detailed Study of Perforated Beams with Closely Spaced Novel Web Openings. In *IABSE Congress Seoul*; 2012; pp. 996–1003.
29. Baddoo, N.R. Stainless steel in construction: A review of research, applications, challenges and opportunities. *J. Constr. Steel Res.* **2008**, *64*, 1199–1206. [CrossRef]
30. Rabi, M.; Cashell, K.A.; Shamass, R. Analysis of concrete beams reinforced with stainless steel. In Proceedings of the fib Symposium 2019: Concrete—Innovations in Materials, Design and Structures, Kraków, Poland, 27–29 May 2019; pp. 690–697.
31. Zhao, O.; Gardner, L.; Young, B. Buckling of ferritic stainless steel members under combined axial compression and bending. *J. Constr. Steel Res.* **2016**, *117*, 35–48. [CrossRef]
32. Rabi, M.; Cashell, K.A.; Shamass, R. Flexural analysis and design of stainless steel reinforced concrete beams. *Eng. Struct.* **2019**, *198*, 109432. [CrossRef]
33. Tsavdaridis, K.D.; Galiatsatos, G. Assessment of cellular beams with transverse stiffeners and closely spaced web openings. *Thin-Walled Struct.* **2015**, *94*, 636–650. [CrossRef]

Disclaimer/Publisher's Note: The statements, opinions and data contained in all publications are solely those of the individual author(s) and contributor(s) and not of MDPI and/or the editor(s). MDPI and/or the editor(s) disclaim responsibility for any injury to people or property resulting from any ideas, methods, instructions or products referred to in the content.